Raman Frequency Shifts for the Rotatory Lattice Mode Close to the Melting Point in Ammonia Solid I

H. Karacali and H. Yurtseven*

Department of Physics, Middle East Technical University, 06531 Ankara, Turkey

Received: March 31, 2005; In Final Form: June 29, 2005

We correlate here the thermal expansivity α_p to the frequency shifts $1/\nu(\partial\nu/\partial P)_T$ for the rotatory lattice (librational) mode in ammonia solid I close to the melting point. This is carried out for the pressures of 0, 1.93, and 3.07 kbar at various temperatures for this solid structure. By obtaining linear plots of α_p versus $1/\nu(\partial\nu/\partial P)_T$ for the pressures studied, we extract the values of the slope dP_m/dT according to our spectroscopic relation. Our calculated values of dP_m/dT can be compared with the experimental ones for ammonia solid I close to the melting point.

1. Introduction

Ammonia has been the subject of many studies in the literature to explain the critical behavior of various physical quantities near the melting point. Since it has a rich phase diagram including solid structures, liquid phases, and also mixture of liquid and solid phases, as shown in the $P-T$[1−3] and $V-T$[2−4] phase diagrams, various physical properties have been studied both experimentally and theoretically.

Some experimental studies include X-ray[5] and neutron scattering,[6] an infrared study,[7] Raman studies on liquid NH_3[8] and on ammonia solids I[9] and II,[10,11] some earlier measurements of the specific heat C_p,[12] molar volume,[13] and the thermal expansivity,[14] and also measurements of the isothermal compressibility.[15,16]

On the basis of the X-ray[5] and neutron scattering[6] experiments, the crystal structures of solid ammonia have been determined. Ammonia solid I has a simple cubic (sc) structure with four molecules per unit cell. Ammonia solids II and III have hexagonal close packed (hcp) and face-centered cubic (fcc) structures, respectively, as reported in an earlier study.[2] It has been shown experimentally that orientational disorder occurs near the melting point in ammonia solid I[17] and a strong orientational disorder occurs in solids II and III of NH_3 and ND_4.[18]

The Raman spectra of ammonia solid I have shown that there are four translational modes of A, E, and 2F and five rotational modes of A, E, and 3F.[4] They are the zone-center lattice modes, and all are Raman-active. For ammonia solid II, the Raman spectra have also shown that there are two lattice frequencies of 54 and 280 cm^{-1} at 219.8 K and 3.07 kbar, which have been assigned as translational modes.[10] Alternatively, those lattice frequencies from the Raman spectra at 65 and 310 cm^{-1} have been assigned as one translational and one rotational, respectively.[3,19]

In ammonia, the solid I phase melts into the liquid state at the melting temperature $T_m = 192.5$ K at zero pressure. This melting occurs in ammonia solid II at $T_m = 222.4$ K at the pressure of 3.07 kbar. From solid I to solid II, a phase transformation takes place at above 3 kbar. Between the melting curves of ammonia solids I and II and between the phase line of those two solid structures, there exists a triple point with the coordinates $T_{l-I-II} = 217.34$ K and $P_{l-I-II} = 3.07$ kbar. There also exits a triple point between the gaseous, liquid, and solid I phases at $T_{g-l-I} = 195.48$ K at zero pressure. Those phases and the points where the phase lines meet have been shown in the experimental $P-T$[1−3] and $V-T$[2−4] phase diagrams, as indicated previously.

They have also been shown in our $P-T$ phase diagrams including the structures of solids I and II[20] and solid III,[21] which we have calculated using the mean field theory. The solid structure, ammonia solid III, has been observed experimentally at 35 kbar and 298 K.[2]

The volume dependence of the Raman frequencies has been studied experimentally in ammonia solid I [4] and solid II.[10,11] Recently, we have calculated the temperature[22] and pressure[23] dependence of the Raman frequencies for two translational and one rotational (librational) modes in ammonia solid I near the melting point. Also, we have calculated the temperature[24] and pressure[25] dependence of the Raman frequencies for the rotatory lattice (librational) mode in ammonia solid II near the melting point.

By consideration of this temperature and pressure dependence of the Raman frequencies in ammonia solids I and II, the Raman frequency shifts can be related to thermodynamic quantities such as the specific heat C_p, thermal expansivity α_p, and the isothermal compressibility κ_T in these crystalline systems close to the melting point. This introduces spectroscopic modification of the Pippard relations, as we have given for ammonium halides in our earlier studies.[27,82] It is based on the critical behavior of ammonia solids I and II near the melting point, as observed experimentally[15,16] and calculated by us.[28] This then led us to apply the Pippard relations to ammonia solids I and II near the melting point.[29]

In this study, we apply a spectroscopic modification of the second Pippard relation (thermal expansivity α_p versus the frequency shifts $1/\nu(\partial\nu/\partial P)_T$) to ammonia solid I, using our calculated Raman frequencies of the rotatory lattice (librational) mode[22] near the melting point.

Section 2 gives a theoretical background for the spectroscopically modified Pippard relation in ammonia solid I. Section 3

* Author to whom correspondence should be addressed. E-mail: karacali@newton.physics.metu.edu.tr.

10.1021/jp058111d CCC: $30.25
Published on Web 08/11/2005

gives our calculations and results. Sections 4 and 5 present our discussion and conclusions, respectively.

2. Theory

A linear relationship between the thermal expansivity α_p and the isothermal compressibility κ_T can be established by means of the Pippard relation for ammonia solid I near the melting point

$$\alpha_p = \left(\frac{dP_m}{dT}\right)\kappa_T + T\left(\frac{dV}{dT}\right)_m \quad (2.1)$$

In this relation, dP_m/dT represents the slope in the $P-T$ phase diagram of ammonia solid I, and $(dV/dT)_m$ is the variation of the solid volume with the temperature at the melting point. The slope dP_m/dT depends on the temperature.

We can modify the above relation spectroscopically for ammonia solid I by defining the isothermal mode Grüneisen parameter

$$\gamma_T = \frac{1}{\kappa_T}\frac{1}{\nu}\left(\frac{\partial\nu}{\partial P}\right)_T \quad (2.2)$$

We then obtain

$$\alpha_p = \frac{1}{\gamma_T}\left(\frac{dP_m}{dT}\right)\frac{1}{\nu}\left(\frac{\partial\nu}{\partial P}\right)_T + \frac{1}{V}\left(\frac{dV}{dT}\right)_m \quad (2.3)$$

This is the spectroscopic modification of the Pippard relation (eq 2.1), which relates the thermal expansivity α_p to the frequency shifts with the pressure, $1/\nu(\partial\nu/\partial P)_T$, for ammonia solid I close to the melting point. By assuming that the mode Grüneisen parameter γ_T remains constant right through the phase transition, a linear variation of the thermal expansivity α_p can be established with the frequency shifts $1/\nu(\partial\nu/\partial P)_T$ according to eq 2.3 near the melting point for ammonia solid I.

To establish eq 2.3, the frequency shifts $1/\nu(\partial\nu/\partial P)_T$ can be calculated from the isothermal compressibility κ_T using eq 2.2 or using the volume data, according to the definition $\kappa_T \equiv -1/V(\partial V/\partial P)_T$. From the frequency shifts calculated, the pressure dependence of the frequency can be obtained as

$$\nu_T(P) = \Delta_T + A(T) + \nu_m \exp\left[-\gamma_T \ln\frac{V_T(P)}{V_m}\right] \quad (2.4)$$

where the additional term is given by

$$A(T) = a_0 + a_1(T_m - T) + a_2(T_m - T)^2 \quad (2.5)$$

for ammonia solid I near the melting temperature T_m. In eq 2.5, a_0, a_1, and a_2 are constants. In eq 2.4, Δ_T is defined as the order−disorder contribution to the frequency with the values of $\Delta_T = 0$ for $P < P_c$ and $\Delta_T \neq 0$ for $P > P_c$. Also, in eq 2.4, ν_m and V_m are the melting frequency of the mode studied and the melting volume, respectively. They have the values of the mode frequency and of the crystal volume at the melting temperature T_m for a constant pressure in ammonia solid I.

The pressure dependence of the volume in ammonia solid I can also be calculated using the power-law formula for the isothermal compressibility given by

$$\kappa_T = k(P - P_m)^{-\gamma} \quad (2.6)$$

due to Pruzan et al.[15] close to the melting point. Here, γ is the critical exponent for the isothermal compressibility κ_T, and k is the amplitude. This then gives the pressure dependence of the crystal volume as

$$V_s = V_c \exp[-k(1-\gamma)^{-1}(P - P_m)^{1-\gamma}] \quad (2.7)$$

where V_c is the critical volume that takes on the values of the crystal volume at various temperatures in the temperature range studied for ammonia solid I.

Close to the melting point in ammonia solid I, the ratio

$$\frac{P - P_m(T)}{T_m(P) - T} = \frac{dP_m}{dT} \quad (2.8)$$

can be considered as an approximate relation.[16] By means of this ratio and eq 2.7, the temperature dependence of the solid volume of ammonia can be written as

$$V_s = V_c \exp\left[-k(1-\gamma)^{-1}\left(\frac{dP_m}{dT}\right)^{1-\gamma}(T_m - T)^{1-\gamma}\right] \quad (2.9)$$

Thus, with the temperature dependence of the critical volume V_c and of the slope dP_m/dT, the volume V_s of ammonia solid I can be predicted close to the melting point, according to eq 2.9. To obtain a linear variation of the thermal expansivity α_p with the frequency shifts $1/\nu(\partial\nu/\partial P)_T$ using eq 2.3, we also require the temperature dependence of α_p, which can be obtained from eq 2.9. This then gives

$$\alpha_p = k\left(\frac{dP_m}{dT}\right)^{1-\gamma}(T_m - T)^{-\gamma} + \frac{1}{V_c}\left(\frac{dV_c}{dT}\right) \quad (2.10)$$

Therefore, by means of eqs 2.10 and 2.4 we can predict the temperature dependence of the thermal expansivity α_p and of the frequency shifts $1/\nu(\partial\nu/\partial P)_T$, respectively, for ammonia solid I near the melting point. Since α_p is related linearly to $1/\nu(\partial\nu/\partial P)_T$, according to eq 2.3, the plot of α_p versus $1/\nu(\partial\nu/\partial P)_T$ allows us to predict dP_m/dT and $1/V(\partial V/\partial T)_m$ from its slope and intercept, respectively.

3. Calculations and Results

We predicted here the temperature dependences of the thermal expansivity α_p and the frequency shifts $1/\nu(\partial\nu/\partial P)_T$ for ammonia solid I near the melting point according to eq 2.3. For the temperature dependence of the thermal expansivity α_p (eq 2.10), we first obtained the temperature dependence of the slope dP_m/dT using the empirical relation

$$P_m(\mathrm{I}) = 5.886\left[\left(\frac{T}{T_{g-l-I}}\right)^{3.96} - 1\right] \quad (3.1)$$

for ammonia solid I due to Pruzan et al.[15] This gives the temperature dependence of the slope dP_m/dT as

$$dP_m(\mathrm{I})/dT = 1.967 \times 10^{-8} T^{2.96} \quad (3.2)$$

We also used the empirical relation

$$V_c(\mathrm{I}) = V_I - d_I(T - T_{g-l-I}) \quad (3.3)$$

for ammonia solid I[15] to obtain the temperature dependence of α_p in eq 2.10. In eq 3.3, the values of $V_I = 21.61$ cm^3/mol and $d_I = 0.0316$ cm^3/mol K[15] were used, which gave us the

TABLE 1: Values of the Coefficients $\Delta_T + a_0$, a_1, and a_2 Determined from Eq 2.4 Using the Volume Values Deduced from Eq 2.9 and the Raman Frequencies of the Rotational Mode of ν_R (280 cm^{-1}) in Ammonia Solid I for the Pressures Indicated[a]

P (kbar)	T_m (K)	$\Delta_T + a_0$ (cm^{-1})	a_1 (cm^{-1}/K)	$a_2 \times 10^{-4}$ (cm^{-1}/K^2)	calculated dP_m/dT (bar/K)	observed dP_m/dT (bar/K)	$-1/V_m(dV_m/dT) \times 10^{-4}$ (K^{-1})	$1/V_c(dV_c/dT) \times 10^{-3}$ (K^{-1})
0	192.5	−9.964	0.1697	5.679	121	113	17.93	1.4557
1.93	210	−13.055	0.1676	3.029	176	147	20.53	1.4938
3.07	217	−14.213	0.1634	3.029	205	162	21.79	1.5095

[a] We give here the values of the slope dP_m/dT that we obtained from the second Pippard relation (eq 2.3) and those values of dP_m/dT deduced from the empirical relation (eq 3.2). The intercept values of $1/V_m(dV_m/dT)$ according to eq 2.3 are tabulated. We also give here the variation of the critical volume with the temperature, $1/V_c(dV_c/dT)$ (eq 3.4).

temperature dependence of the critical volume V_c as

$$V_c(\mathrm{I}) = 27.79 - 0.0316T \qquad (3.4)$$

with the value of $T_{g-l-I} = 195.48$ K.

We were then able to correlate the thermal expansivity α_p to the Raman frequency shifts $1/\nu(\partial\nu/\partial P)_T$ of the librational mode of ν_R (280 cm^{-1}) in ammonia solid I, according to the second Pippard relation (eq 2.3) for the fixed pressures of 0, 1.93, and 3.07 kbar. For this correlation, we first calculated the Raman frequencies of this mode through the relation (eq 2.4) where we used the volume values deduced from the pressure dependence of the solid volume V_s (eq 2.7) in ammonia solid I. In eq 2.7, the critical volume V_c was obtained from the empirical relation (eq 3.4). By using the values of the amplitude $k = 0.0137$ and the critical exponent $\gamma = 0.49$ for ammonia solid I according to eq 2.6,[15] we were able to determine the pressure dependence of the solid volume V_s (eq 2.7) in this crystalline system. Those values of the solid volume were used in eq 2.4 to predict the Raman frequencies of the librational mode ν_R (280 cm^{-1}) with the values of volume $V_m = 21.61$ cm^3/mol and the Raman frequency of $\nu_m = 276.31$ cm^{-1} of the librational mode at the melting temperature T_m. The value of the Grüneisen parameter of this mode was taken as $\gamma_T = 0.8$[4] in this relation. Since eq 2.4 includes the temperature-dependent term $A(T)$ with the coefficients a_0, a_1, and a_2 (eq 2.5), we determined the coefficients $\Delta_T + a_0$, a_1, and a_2 by using eq 2.4 where the volume values as a function of pressure were used, according to eq 2.7. In fact, for those three coefficients, we used three observed values of the frequency for the librational mode[4] at three different temperatures for each fixed pressure. Therefore, we obtained three sets of those coefficients $\Delta_T + a_0$, a_1, and a_2 at three different temperatures for fixed pressures of 0, 1.93, and 3.07 kbar in ammonia solid I, as given in Table 1. By means of the pressure dependence of the solid volume V_s (eq 2.7) and the values of those coefficients, the pressure dependence of the Raman frequencies of the librational mode was then obtained according to eq 2.4. From this relation, we were able to obtain the values of the frequency shifts $1/\nu(\partial\nu/\partial P)_T$ at various temperatures for the fixed pressures of 0, 1.93, and 3.07 kbar in ammonia solid I, which we used in the second Pippard relation (eq 2.3).

For the second Pippard relation, we also needed the values of the thermal expansivity α_p at various temperatures for the fixed pressures considered in ammonia solid I, which were deduced using eq 2.10. For this, the values of the slope dP_m(I)/dT were obtained from the empirical relation (eq 3.2), as indicated previously, as a function of temperature for the pressures, namely, 0, 1.93, and 3.07 kbar. In eq 2.10, the variation of the critical volume V_c with the temperature, $1/V_c(dV_c/\partial T)$, was obtained at the melting temperature according to eq 3.4, whose values are given in Table 1. Thus, with the same values of γ and k, we obtained the temperature dependence of the thermal expansivity α_p (eq 2.10). Now, with the values of

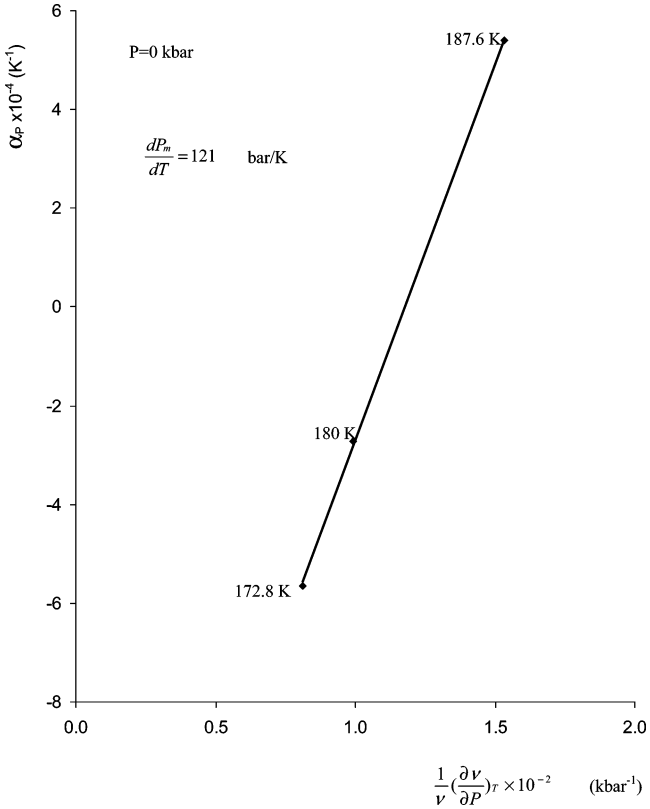

Figure 1. Thermal expansivity α_p as a function of the Raman frequency shifts $1/\nu(\partial\nu/\partial P)_T$ for the rotatory (librational) mode of ν_R (280 cm^{-1}) in ammonia solid I for $P = 0$ kbar ($T_m = 192.5$ K).

the Raman frequency shifts of the librational mode of ν_R (280 cm^{-1}) and those values of the thermal expansivity α_p, we established the second Pippard relation (eq 2.3) at various temperatures close to the melting point for the fixed pressures of 0, 1.93, and 3.07 kbar in ammonia solid I. Figures 1−3 give our plots of α_p versus $1/\nu(\partial\nu/\partial P)_T$ for the pressures of 0, 1.93, and 3.07 kbar, respectively. From our plots, we deduced the values of the slope dP_m/dT and also the values of the intercept $1/V_m(dV_m/\partial T)$ for the fixed pressures considered in ammonia solid I. Those values are listed in Table 1 where we also give the values of dP_m/dT, which we deduced from the empirical relation (eq 3.2) for comparison.

4. Discussion

As given in Figures 1−3, we obtained linear plots of the thermal expansivity α_p versus the Raman frequency shifts for the ν_R (280 cm^{-1}) rotatory lattice (librational) mode in ammonia solid I near the melting point. Our plots (Figures 1−3) were obtained for the pressures of 0, 1.93, and 3.07 kbar, respectively, in this crystal system. From our plots, which did not include many data points because of the lack of the observed Raman data that we used,[4] we attempted to extract the values of the

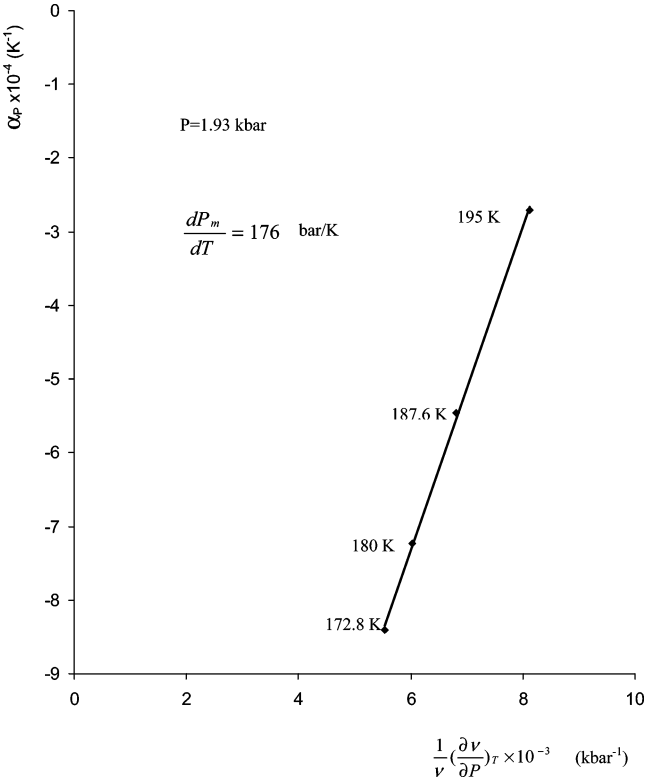

Figure 2. Thermal expansivity α_p as a function of the Raman frequency shifts $1/\nu(\partial\nu/\partial P)_T$ for the rotatory (librational) mode of ν_R (280 cm^{-1}) in ammonia solid I for $P = 1.93$ kbar ($T_m = 210$ K).

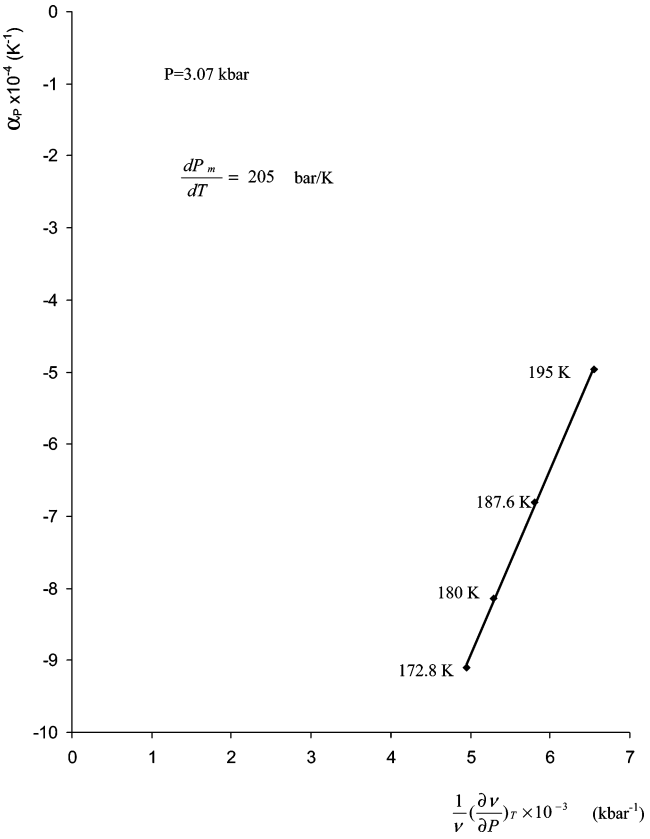

Figure 3. Thermal expansivity α_p as a function of the Raman frequency shifts $1/\nu(\partial\nu/\partial P)_T$ for the rotatory (librational) mode of ν_R (280 cm^{-1}) in ammonia solid I for $P = 3.07$ kbar ($T_m = 217$ K).

slope dP_m/dT, as given in Table 1 with the experimental values for comparison. Our calculated value of 121 bar/K for zero pressure is not far from the observed value of 113 bar/K. However, as the pressure increases, the discrepancy increases, and it seems that there is no agreement between our calculated and observed values (Table 1). On the basis of our assumptions made for our spectroscopic modification of the Pippard relation (eq 2.3) and for the mode Grüneisen parameter (eq 2.2), this discrepancy between our calculated and observed values of dP_m/dT may be explained. First, we assumed that the Raman frequency shifts $1/\nu(\partial\nu/\partial P)_T$ for this rotatory lattice (librational) mode have a similar divergence behavior as the thermal expansivity α_p exhibits in ammonia solid I near the melting point. This divergence behavior of $1/\nu(\partial\nu/\partial P)_T$ may then be different from that of the thermal expansivity α_p. Second, we assumed that according to eq 2.2 the isothermal mode Grüneisen parameter γ_T for this rotatory mode remains constant right through the phase transition near the melting point in ammonia solid I. This leads us to describe the critical behavior of the frequency shifts $1/\nu(\partial\nu/\partial P)_T$, the same as that of the isothermal compressibility κ_T (eq 2.2) in ammonia solid I near the melting point.

Regarding the Raman frequencies of the rotatory lattice (librational) mode in ammonia solid I, our spectroscopic relation (eq 2.3) is applicable satisfactorily for zero pressure with a constant mode Grüneisen parameter γ_T (Figure 1). As the pressure increases, application of our relation (eq 2.3) does not describe satisfactorily the observed behavior of ammonia solid I. This may be due to the fact that the mode Grüneisen parameter γ_T depends on the pressure and temperature near the melting point in ammonia solid I. This may then cause the decrease in the discrepancy between our calculated and the observed values of dP_m/dT at higher pressures in ammonia solid I.

Once our spectroscopic modification of the second Pippard relation (eq 2.3) is validated, the critical behavior of the thermal expansivity α_p (eq 2.10) and of the isothermal compressibility κ_T (eq 2.6) can be predicted from the Raman frequency shifts $1/\nu(\partial\nu/\partial P)_T$ in ammonia solid I near the melting point. In this case, α_p and κ_T can be predicted using our calculated Raman frequency shifts $1/\nu(\partial\nu/\partial P)_T$ for the rotatory lattice (librational) mode of ν_R (280 cm^{-1}) in ammonia solid I. This then provides the thermodynamic data for the α_p and κ_T, which can be collected by means of the spectroscopic measurements, according to our relation (eq 2.3). Since the Raman frequencies can be measured to a high accuracy compared to the thermodynamic data, which are not easily obtainable, our spectroscopic modification of the second Pippard relation (eq 2.3) can be used satisfactorily to explain the observed behavior of an ammonia solid system near the melting point. It can also be applied to those systems exhibiting similar phase transitions as exhibited by the ammonia solid system near the melting point.

5. Conclusions

We applied here our spectroscopic modification of the Pippard relation to ammonia solid I by using our calculated Raman frequencies for the rotatory lattice (librational) mode in this system close to the melting point. From this application, we obtained a linear variation of the thermal expansivity α_p with the Raman frequency shifts $1/\nu(\partial\nu/\partial P)_T$ for the pressures of 0, 1.93, and 3.07 kbar in this crystalline system. The values of the slope dP_m/dT that we extracted from those linear plots were compared with the experimental values.

References and Notes

(1) Hanson, R. C.; Jordan, M. *J. Phys. Chem.* **1980**, *84*, 1173.
(2) Mills, R. L.; Liebenberg, D. H.; Pruzan, Ph. *J. Phys. Chem.* **1982**, *86*, 5219.

(3) Gauthier, M.; Pruzan, Ph.; Besson, J. M.; Havel, G.; Syfosse, G. *Physica B+C* **1986**, *139−140*, 218.
(4) Nye, C. L.; Medina, F. D. *Phys. Rev. B* **1985**, *32*, 2510.
(5) Olovsson, I.; Templeton, D. H. *Acta Crystallogr.* **1959**, *12*, 832.
(6) Reed, J. W.; Harris, P. M. *J. Chem. Phys.* **1961**, *35*, 1730.
(7) Bromberg, A.; Kimel, S.; Ron, A. *Chem. Phys. Lett.* **1977**, *46*, 262.
(8) Lundeen, J. W.; Koehler, W. H. *J. Chem. Phys.* **1975**, *79*, 2957.
(9) Nye, C. L.; Medina, F. D. *Phys. Rev. B* **1985**, *32*, 2510.
(10) Luo, R. K.; Nye, C.; Medina, F. D. *J. Chem. Phys.* **1986**, *85*, 4903.
(11) Luo, R. K.; Medina, F. D. *Phys. Rev. B* **1990**, *42*, 3190.
(12) Overstreet, R.; Giange, W. F. *J. Am. Chem. Soc.* **1937**, *59*, 254.
(13) Manzhelii, V. G.; Tolkachev, A. M. *Sov. Phys. Solid State* **1964**, *5*, 2506.
(14) Manzhelii, V. G.; Tolkachev, A. M. *Sov. Phys. Solid State* **1966**, *8*, 827.
(15) Pruzan, Ph.; Liebenberg, D. H.; Mills, R. L. *Phys. Rev. Lett.* **1982**, *48*, 1200.
(16) Pruzan, Ph.; Liebenberg, D. H.; Mills, R. L. *J. Phys. Chem. Solids* **1986**, *47*, 949.
(17) Hewat, A. W.; Rickel, C. *Acta Crystallogr., Sect. A* **1979**, *35*, 569.
(18) Eckert, J.; Mills, R.; Satija, S. *J. Chem. Phys.* **1985**, *81*, 6034.
(19) Gauthier, M.; Pruzan, Ph.; Chervin, J. C.; Besson, J. M. *Phys. Rev. B* **1988**, *37*, 2102.
(20) Salihoğlu, S.; Tarı, Ö.; Yurtseven, H. *Phase Transitions* **2000**, *72*, 299.
(21) Enginer, Y.; Salihoğlu, S.; Yurtseven, H. *Mater. Chem. Phys.* **2002**, *73*, 57.
(22) Yurtseven, H. *J. Phys. Chem. A* **1999**, *103*, 5900.
(23) Yurtseven, H. *Acta Physica Pol., A* **2001**, *99*, 557.
(24) Yurtseven, H.; Ugur, S. *Chin. J. Phys.* **2003**, *41*, 140.
(25) Yurtseven, H. *Chin. J. Phys.* **2004**, *42*, 209.
(26) Yurtseven, H.; Sherman, F. W. *J. Mol. Struct.* **1994**, *323*, 243.
(27) Yurtseven, H.; Sherman, F. W. *J. Mol. Struct.* **1997**, *435*, 143.
(28) Yurtseven, H.; Salihoglu, S. *Chin. J. Phys.* **2002**, *40*, 416.
(29) Yurtseven, H. *Int. J. Mod. Phys. B* **1999**, *13*, 2783.